

Vibrationally elastic scattering of electrons by HCl

N. T. Padiyal* and D. W. Norcross†

*Joint Institute for Laboratory Astrophysics, University of Colorado
and National Bureau of Standards, Boulder, Colorado 80309*

L. A. Collins

Group T4, Mail Stop 212, Los Alamos National Laboratory, Los Alamos, New Mexico 87545

(Received 25 March 1982)

Results of close-coupling calculations are reported, in which several models of the interaction potential are investigated. Cross sections for rotational transitions involving the lowest ten levels are obtained in the first detailed application of the MEAN approximation. The results are subject to a strong cooperative effect involving exchange and polarization. Rotationally elastic transitions are shown to be quite important at thermal energies and to dominate the total cross section above 4.0 eV. Transitions for which the angular momentum changes by two are found to be responsible for a broad resonance at ~ 2.5 eV. No structure indicative of a resonance or virtual state at very low energies is, however, obtained. Total differential, momentum-transfer, and integrated cross sections are in satisfactory agreement with measured values.

I. INTRODUCTION

The study of electron scattering by HCl has a long and interesting history. It was one of the first polar molecules to which close-coupling techniques were applied.^{1,2} It was also one of the first polar molecules for which a fascinating resonance structure in vibrational excitation was revealed.³ These measurements, complemented by others of dissociative attachment and associative detachment, stimulated a vigorous debate in an effort to develop a coherent physical picture of the collision process.⁴ A central feature of this debate concerns the significance of the polar nature of the molecule in the interpretation of these measurements, and it remains controversial.⁵ The large vibrational excitation cross sections measured earlier,⁶ coupled with recent measurements⁷ of enhanced attachment rates for excited vibrational states, cannot be easily rationalized with the surprisingly weak rates for attachment⁸ and vibrational excitation⁹ measured upon dumping a high-energy pulse of electrons into the gas.

In the hope of making a contribution to the understanding of these various results, we have undertaken a detailed computational study of electron scattering by HCl. We report here results of the first stage of these calculations—for rotational transitions in vibrationally elastic scattering. There is now a wealth of experimental data available for various aspects of this process: total cross sec-

tions,¹⁰ differential cross sections,⁶ and momentum-transfer cross sections.¹¹ These data provide invaluable benchmarks on the way to a successful *ab initio* treatment of the more complicated vibrational excitation and attachment-detachment processes.

The interaction potential, and approaches to the solution of the scattering equations and to the evaluation of cross sections are first briefly described. The various parameters have been carefully chosen to ensure that the accuracy of the results is limited primarily by the physical approximations made, not by the precision of the calculations. Our results are then summarized, conclusions drawn, and future work outlined.

II. MODEL OF THE INTERACTION POTENTIAL

Our study uses as its primary vehicle a near-Hartree-Fock wave function for HCl.¹² The static interaction potential is obtained using new computer codes for expanding the electronic charge distribution¹³ and for using this to produce a Legendre expansion of the potential.¹⁴ The exchange interaction, which is known¹⁵ to be an important effect in low-energy scattering by HCl, is included using the free-electron-gas approximation.¹⁶ This model of the interaction potential is denoted SME, for static-model-exchange. Some of the most important details of this model include the number of terms taken in the expansion of the nuclear, static electronic,

and exchange interaction (at least 34, 17, and 17, respectively) and the equilibrium values of the dipole and quadrupole moments obtained (-0.470 and -2.826 a.u., respectively), which compare quite favorably with measured values (-0.436 and -2.778 a.u., respectively) for the ground vibrational state.¹⁷

Polarization, which has also been shown¹⁸ to be an important effect for HCl, is included via a local form correct at large radii, but employing a cutoff function with one adjustable parameter at short radii. This is probably the weakest part of our current model of the interaction potential. The experimental values of the spherically symmetric and quadrupole static polarizabilities used are 17.41 (Ref. 19) and 1.40 a.u.,²⁰ respectively, and the polarization potential is taken to have the form

$$V_{\text{pol}}(r) = -\frac{1}{2} \left[\frac{\alpha_0}{r^4} + \frac{\alpha_2}{r^2} P_2(\theta) \right] (1 - e^{-(r/r_c)^6}), \quad (1)$$

where the distance of the H atom from the center-of-mass ($2.34a_0$) is used for the cutoff radius r_c . Models employing this interaction are denoted, for example, SMEP.

We also consider, in addition to the SME and SMEP models, several other approximations: static (S), static-polarization (SP), adding to the SME potential the requirement of orthogonality of all bound and continuum orbitals (OSME),²¹ and an essentially exact solution of the scattering equations in the static-exchange approximation (ESE) using the linear-algebraic formulation.²²

III. SOLUTION OF THE SCATTERING EQUATIONS

The scattering equations are solved using an integral equations formulation of the close-coupling approximation for electron-molecule scattering.²³ All calculations are carried out at the equilibrium internuclear separation and in the molecular body-fixed (BF) coordinate frame with the fixed-nuclei (FN) approximation, i.e., the rotational and vibrational Hamiltonians are neglected. Typically, 18 channels are retained in the coupled equations. The inclusion in the coupled equations of channels with high angular momentum is required only for the purpose of converging the calculation in the vicinity of the nuclei—only the lowest five or six channels carry any significant amount of flux from the inner to asymptotic region.

Reactance matrices are extracted by matching to plane waves upon propagation to a radius of at least $150/k a_0$, where k^2 is the collision energy in rydbergs. This ensures that the contribution from the dipole interaction to all channels included in the scattering equations, which is confined to large radii for large angular momenta, is accounted for completely. In Table I we compare reactance matrices elements calculated using integration radii of $\sim 150/k$ and 100.0 bohr at the energies of 0.01, 0.1, and 0.3 eV in the SP model. For the smaller energies even the very low angular momenta R -matrix elements are not well converged at 100.0 bohr (convergence of elements for higher angular momenta is, of course, much worse at $100.0a_0$).

We could, alternatively, have demanded good con-

TABLE I. Reactance matrix elements (Σ symmetry) calculated with different ranges of integration (R_{max}) in the SP model.

l	l'	$E=0.01$ eV		$E=0.1$ eV		$E=0.3$ eV	
		$R_{\text{max}}=100.0$	$R_{\text{max}}=6040.0$	$R_{\text{max}}=100.0$	$R_{\text{max}}=1540.0$	$R_{\text{max}}=100.0$	$R_{\text{max}}=1140.0$
0	0	0.174(0) ^a	0.226(0)	0.480(-1)	0.633(-1)	-0.129(0)	-0.121(0)
0	1	0.282(0)	0.270(0)	0.273(0)	0.275(0)	0.261(0)	0.264(0)
0	2	0.236(-1)	0.797(-2)	0.227(-1)	0.187(-1)	0.331(-1)	0.308(-1)
0	3	0.105(-2)	0.961(-3)	0.156(-2)	0.119(-2)	0.175(-2)	0.143(-2)
0	4	0.242(-4)	0.327(-4)	0.129(-3)	0.963(-4)	0.194(-3)	0.175(-3)
1	1	0.131(-1)	-0.283(-1)	0.101(-1)	0.187(-3)	-0.104(-1)	-0.154(-1)
1	2	0.641(-1)	0.123(0)	0.117(0)	0.121(0)	0.115(-1)	0.116(0)
1	3	0.275(-2)	0.173(-2)	0.737(-2)	0.563(-2)	0.104(-1)	0.949(-2)
1	4	0.546(-4)	0.201(-3)	0.328(-3)	0.255(-3)	0.424(-3)	0.359(-3)
2	2	0.488(-2)	-0.226(-2)	0.111(-1)	0.948(-2)	0.273(-1)	0.265(-1)
2	3	0.101(-1)	0.799(-1)	0.762(-1)	0.797(-1)	0.787(-1)	0.799(-1)
2	4	0.233(-3)	0.864(-3)	0.381(-2)	0.269(-2)	0.530(-2)	0.469(-2)
3	3	0.420(-3)	-0.263(-3)	0.545(-2)	0.465(-2)	0.116(-1)	0.113(-1)
3	4	0.963(-3)	0.594(-1)	0.506(-1)	0.593(-1)	0.569(-1)	0.595(-1)
4	4	0.212(-4)	0.109(-3)	0.282(-2)	0.281(-2)	0.638(-2)	0.632(-2)

^aThe numbers in parentheses indicate the power of 10 that multiplies each element.

vergence of only the lowest five or six channels, perhaps dropping the higher channels beyond the range of most of the molecular charge density, and incorporated the effect of the latter in the collision cross section as described in Sec. IV. This would have reduced the required convergence radius by about a factor of 3, but it would still be more than $100a_0$ for $E \leq 3.0$ eV.

IV. EVALUATION OF CROSS SECTIONS

All cross sections have been evaluated using the multipole-extracted adiabatic-nuclei (MEAN) approx-

$$\Delta \frac{d\sigma(j \rightarrow j')}{d\Omega} = \frac{k_{j'}}{4k_j} \sum_{l_t} C(j, l_t, j'; 00)^2 \frac{1}{k^2} \sum_{\lambda} (B_{\lambda, l_t} - B_{\lambda, l_t}^{FBA}) P_{\lambda}(\theta), \quad (3)$$

the first term in (2) is the appropriate closed-form expression for the particular cross section in the laboratory-fixed coordinate frame in the first Born approximation (FBA),²⁵ and the second term in (3) is the partial-wave representation of the same cross section in the BF frame with the FN approximation. The index l_t denotes the units of angular momenta exchanged during the collision and $C(\dots)$ is a Clebsch-Gordan coefficient.

Given (2) and (3), the corresponding forms of the integral and momentum transfer cross sections are obvious. The form for the energy-loss cross section is obtained²⁶ by simply inserting the factor $l_t(l_t + 1)B$ in (3), for B the rotational constant, with the appropriate form for the first term in (2). In all cases the dependence on initial rotor state is confined to this term and the kinematic ratio and algebraic factor in (3).

The initial (k_j) and final ($k_{j'}$) momenta of the electron are related by

$$k_j^2 - k_{j'}^2 = B[j'(j' + 1) - j(j + 1)], \quad (4)$$

where the rotational constant $B = 1.294$ meV. The coefficients B_{λ, l_t} in (3) are obtained for a range of values of k^2 corresponding to BF-frame energies between 0.003 and 11.0 eV and the results are interpolated on a natural cubic spline to any desired energy defined by (4) and the geometric mean $k^2 = k_j k_{j'}$. The evaluation of the coefficients B_{λ, l_t} is made very efficiently by exploiting the concept²⁴ of the l_t -reduced T matrix, i.e.,

$$T_{l_t, l_t}^m = \sum_m (-1)^m C(l_t, l_t; m, -m) T_{l_t}^m, \quad (5)$$

where m corresponds to the collision symmetry.

In the evaluation of (5), the results of close-

imation.²⁴ In the present application of the MEAN approximation, the partial differential cross section for the transition from initial state j to final state j' is expressed

$$\frac{d\sigma(j \rightarrow j')}{d\Omega} = \frac{d\sigma^{FBA}(j \rightarrow j')}{d\Omega} + \Delta \frac{d\sigma}{d\Omega}(j \rightarrow j'), \quad (2)$$

where

coupling calculations for the lowest five collision symmetries (Σ - Γ) are augmented by unitarized Born (BII) T -matrix elements²⁷ for all angular momenta $l \leq l_b = 55$ (40) for l_t even (odd). BII T -matrix elements are also used for all symmetries above Γ with these angular momenta. The FBA is used for all higher symmetries and angular momenta. The sum in (3) is typically taken up to $\lambda_{\max} = (27, 19, 27, 19, 14, 14)$ for $l_t = (0, \dots, 5)$. Use of the calculated values of the dipole and quadrupole moments, and quadrupole polarizability, in the second term in (3) ensures that the high angular momentum contributions from the two terms cancel identically for $l > l_b + \lambda_{\max}$. Use of the experimental values of the same quantities in the first term in (2) serves to partially correct for the errors in the Hartree-Fock wave function.

IV. RESULTS

Figure 1 shows the eigenphase sum for Σ symmetry for several models of the interaction potential. The logarithmic plot is designed to emphasize the low-energy behavior, in which there is no significant change from the static (S) result until *both* exchange and polarization are included (SMEP). There is no indication of any resonance behavior below 0.5 eV, contrary to the predictions of stabilization calculations,²⁸ or the steep rise to low energies required in the model of Domcke and Cederbaum.⁵ Neither is there anything which might be suggestive of a virtual state, as postulated by Dube and Herzenberg²⁹ and as offered as an interpretation of the stabilization results by Nesbet.³⁰

The eigenphase sum does not go to any multiple of π , irrespective the existence of bound states, as k^2 goes to zero. This limit, in the FN approximation,

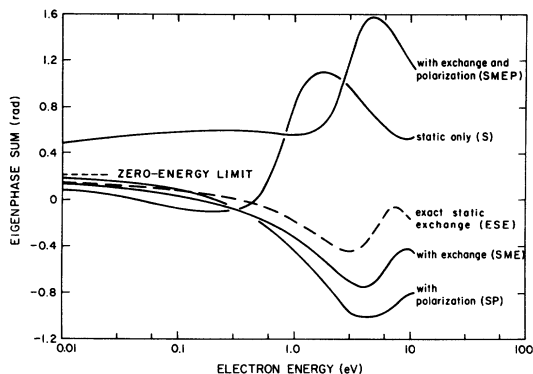


FIG. 1. Fixed-nuclei Σ eigenphase sum versus electron energy for several models of the interaction potential. The dashed line at the left indicates the zero-energy limit for the point-dipole potential.

for a molecule with a dipole moment less than the critical value (0.639 a.u.) is a constant, the value of which is a function solely of the dipole moment. This value can be specified by considering the eigenvalues $N(N+1)$ of the dipole plus angular momentum interaction³¹ and generalizing the solution³² for a central attractive r^{-2} interaction. The result³³ is the sum of the phase shifts for each element of the diagonalized interaction, i.e., $\pi \sum (l-N)/2$. This yields 0.212 for HCl and is consistent with the trend of the results in Fig. 1. It is clear, however, that 0.01 eV is still well above the zero-energy limit, where short-range interactions and those of higher multipolarity can be neglected. Full inclusion of the rotational dynamics in the scattering calculations would result, of course, in the eigenphase sum going to some exact multiple of π , but deviation from the qualitative shape shown in Fig. 1 may not occur until the collision energy is comparable to the characteristic rotational spacing.

At higher energies the inclusion of polarization and exchange separately results in significant change from the result of the S model, and the inclusion of both induces resonance behavior in the energy range 1.0–3.0 eV, as previously noted.¹⁸ Some sensitivity to the choice of r_c (variation of the eigenphase sum approximately linear in r_c for small changes) was noted, but we made no attempt to further tune the choice of r_c based on the observed⁶ resonance position. Results using the OSME model are indistinguishable from the SME curve. Results from the ESE calculations are slightly, but noticeably, different from the SME results at the higher energies, but it remains to be seen what effect this may have on cross sections.

Total (summed over all final rotational states) integrated cross sections are shown in Fig. 2. The

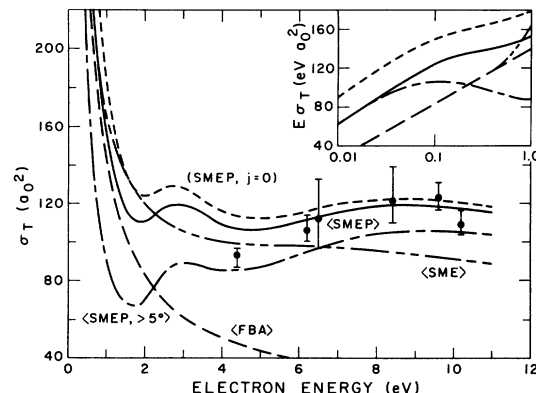


FIG. 2. Total integrated cross sections versus electron energy. The brackets $\langle \rangle$ indicate an average over the thermal distribution of rotational states at 300 K, $j=0$ indicates the cross section for the ground rotational state, $>5^\circ$ indicates that scattering in the angular range $0-5^\circ$ has been neglected, and the FBA curve includes both dipole and quadrupole contributions. The measured data are from Brüche (Ref. 10).

cross section averaged over the distribution of rotational levels at 300 K (for which the most probable rotor state has $j=3$) is strictly required for comparison with the measured values.¹⁰ This is particularly easy in the MEAN approximation, as the sum of (3) over j' is quite insensitive to j above 0.02 eV. Partial integrated cross sections are shown in Fig. 3. The main features of the total cross section are controlled by the term in (3) with $l_i=0$. Only at ~ 1.0 eV, where this contribution becomes small, does the term with $l_i=1$, i.e., the direct dipole transition, dominate the SMEP results. The total integrated cross sections from the SME model is, however, dominated by the dipole interaction below ~ 1.0 eV,

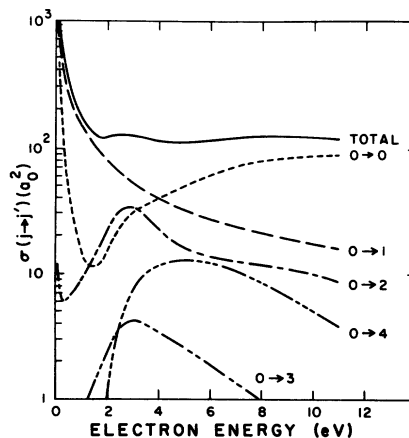


FIG. 3. Partial integrated cross sections for transitions from the ground rotational state versus electron energy.

and comes into agreement with the FBA. The steep rise in the $j=0 \rightarrow 0$ cross section at low energies and the maximum in the $j=0 \rightarrow 2$ cross section at ~ 3.0 eV arise only in the SMEP model. Illustrative results from the SP and SMEP models and from the FBA are given in Tables II and III.

The total momentum-transfer cross section is shown in Fig. 4. Unlike the total integrated cross section, it is quite insensitive to the rotational temperature. The results of the SP and SME models are both in good agreement with the FBA below ~ 1.0 eV. Preliminary analysis of swarm measurements¹¹ yields results that are in remarkably good agreement with the SMEP results over the entire energy range shown. These results are, for example, almost constant at $\sim 65 \text{ eV } a_0^2$ between 0.01 and 0.4 eV, and they qualitatively confirm the minimum around 1.0 eV and rise to higher energies. The good agreement at low energies is particularly satisfying, since it is here that our dynamical approximation is most severely tested.

Total differential cross sections are shown in Fig. 5. These results are also insensitive to rotational temperature from angles greater than a few degrees and energies above a few tenths of eV. The results of the relative measurements⁶ have been normalized to the results of the SMEP model by a single factor that is independent of both energy and angle. The interaction of polarization and exchange is clearly responsible for the resonance feature at ~ 2.5 eV, although it is more pronounced in the calculated results. We also note a significant increase in the cross section at low energies for all but small-angle scattering due to polarization. The results from the various models come into agreement with the FBA only for very small-angle scattering at energies of order a few tenths of an electron volt, and even then differences of order 15% are noted.

The total energy-loss cross section (thermally averaged over the rotational distribution at 300 K)

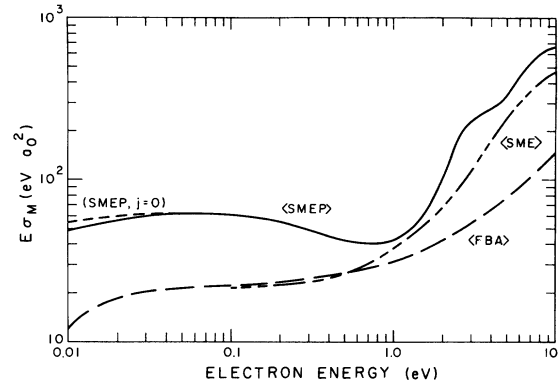


FIG. 4. Total momentum transfer cross sections versus electron energy. Notation is as in Fig. 2.

differs little from the prediction of the FBA for energies below 1.0 eV, but increases, relatively, to be about four times larger at 5.0 eV, then falls again to about a factor of 2 larger for $E \sim 11.0$ eV. This increase relative to the FBA is due primarily to contributions with $l_i=2$ and 4, as might be suspected from Fig. 3.

Detailed and compact tables of partial and total integrated, momentum transfer, and energy-loss cross sections for transitions among the first ten rotational levels over the energy range 0.01–11.0 eV are available on request. Tabulations of partial and total differential cross sections are also available.

VI. DISCUSSION AND CONCLUSIONS

The experimental technique used by Brüche¹⁰ to measure the total integrated cross sections cannot distinguish electrons scattered into some small, ill-defined, angular region in the forward direction from the unscattered beam. Neglecting the contribution from the first 5° , for example, somewhat improves the agreement in shape for the results of the

TABLE II. Cross sections for transitions from state $j=0$. Columns labeled IT and GR are from Refs. 1 and 35, respectively, and those labeled SP and SMEP are described in the text.

E (eV)	$\sigma(0 \rightarrow 0)$				$\sigma(0 \rightarrow 1)$				$\sigma(0 \rightarrow 2)$			
	IT	GR	SP	SMEP	IT	GR	SP	SMEP	IT	GR	SP	SMEP
0.01	421	9600 ^b	895	4320	4960	602 ^a	4970	4600	45.8 ^a	15.7 ^a	147	151
0.03	101	5400 ^b	201	1610	2400	729	2560	2420	24.4 ^a	62.8 ^a	45.5	44.2
0.06	31.4 ^a	2400 ^b	64.6	812	1400 ^a	686 ^a	1550	1480	13.3 ^a	88.9 ^a	22.9	20.5
0.10	9.71	1600 ^b	27.4	470	955	618 ^a	1040	1010	7.57 ^a	102 ^a	14.8	12.0
0.14	4.94 ^a	1040 ^a	19.4	319	703 ^a	560 ^a	794	778	4.88 ^a	106 ^a	11.9	8.9
0.20	4.94 ^a	576 ^a	24.1	205	534 ^a	482 ^a	592	588	3.21 ^a	109 ^a	12.1	7.01
0.30	10.1	314 ^a	44.6	118	383	418	420	424	1.79 ^a	96.9 ^a	18.7	6.16
0.40	15.9 ^a	199 ^a		76.4	314 ^a	377 ^a		335	1.17 ^a	84.8 ^a		6.13

^aExtracted from plot.

^bInterpolated using Figs. 3 and 5 of Ref. 35.

TABLE III. Cross sections for transitions from state $j=0$. Columns labeled AD are from Ref. 36, and those labeled SMEP and FBA are described in the text.

E (eV)	$\sigma(0 \rightarrow 0)$		$\sigma(0 \rightarrow 1)$			$\sigma(0 \rightarrow 2)$		
	AD	SMEP	AD	SMEP	FBA	AD	SMEP	FBA
0.01	960	4320	6020	4600	5620	451	151	4.11
0.03	320	1610	2800	2420	2740	150	44.2	7.55
0.06	160	812	1650	1480	1630	75.2	20.5	8.25
0.1	96.0	470	1100	1010	1090	45.1	12.0	8.56
0.3	32.0	118	446	424	443	15.0	6.16	9.01
0.6	16.0	38.9	248	239	247	7.52	6.79	9.29
1.0	9.60	15.8	160	155	159	4.51	9.06	9.53
3.0	3.20	31.0	61.2	51.9	61.0	1.50	33.1	10.3
6.0	1.60	60.7	33.1	27.4	33.0	0.752	13.5	11.1
10.0	0.960	88.1	21.0	17.6	21.0	0.451	9.79	11.8

SMEP model, but a similar correction for the results of the SME model would clearly lead to worse agreement. Since 5° is probably too low an estimate for the angular resolution (15° might be closer to the truth), the agreement of calculated and measured cross sections is not as good as it might at first appear. Bruche suggests, however, that the more correct results may correspond to the lower limits of the plotted uncertainties, since the data taken was subject to unexplained monotonic upward drift.

The importance of the contribution from small-angle scattering is also relevant to attempts to obtain the total integrated cross section by extrapolating measurements of differential cross sections made over a finite angular range. The contribution to the SMEP results from the angular ranges below 15° and above 120° is, for example, between 37% and 66% of the total over the energy range 0.3–11.0 eV. The cross sections for vibrational excitation measured by Rohr and Linder⁶ were put on an absolute scale by extrapolating the measured differential cross sections for vibrationally elastic scattering to

0° and to 180° , integrating, and normalizing to the measured¹⁰ integrated cross section in the vicinity of 10.0 eV. The fact that the present results also agree (fortuitously, as noted) with the measured¹⁰ total integrated cross section, but that a further renormalization of the measured⁶ differential cross sections by a factor of 0.7 is required, suggests that the contribution from small- and large-angle scattering has been underestimated in the experimental analysis. This normalization factor is consistent with the error estimates adopted by Rohr and Linder⁶ and also with the results of the swarm analysis,¹¹ in which a reduction of the vibrational excitation cross sections by about a factor of 2 was required.

Speculating on the basis of the present results, we suspect that the sharp near-threshold peak observed⁶ in vibrational excitation may be a consequence not of any low-energy resonance or virtual state, but of the finite nature of the eigenphase sum coupled with an increasing sensitivity to internuclear separation at low energies induced by the interaction of polarization and exchange. Rescigno *et al.*³⁴ reached a simi-

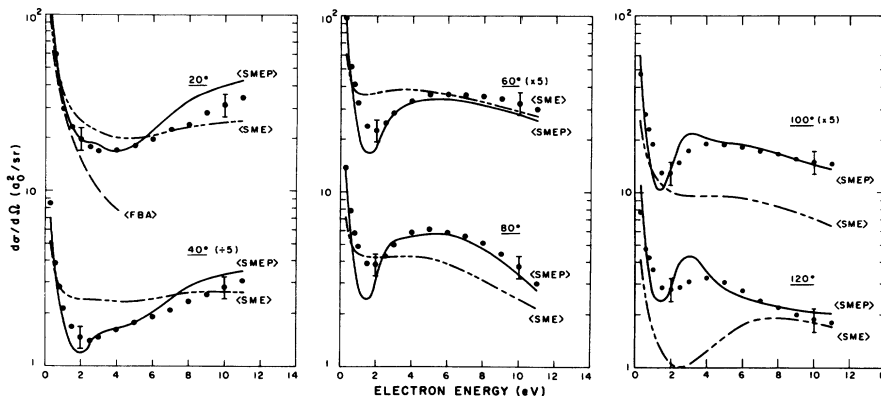


FIG. 5. Total differential cross sections versus electron energy. Notation is as in Fig. 2. The measured data are from Rohr and Linder (Ref. 6).

lar conclusion in their study of HF. If so, this will preclude generalization to the whole class of polar molecules, or even to the hydrogen halides. Perhaps only full vibrational close-coupling calculations will resolve this question.

The broader and weaker maximum in the observed vibrational excitation cross section around 2.5 eV is almost certainly associated with the maximum in the $0 \rightarrow 2$ cross section seen in Fig. 3, i.e., with transitions for which $l_i = 2$. As noted earlier, the energy loss associated with transitions for which $l_i > 1$, is substantial above 1.0 eV, yielding a total that is $\sim 30\%$ of that due to vibrational excitation. It may be partially responsible, through more rapid than expected electron cooling, for the surprisingly low attachment and vibrational excitation rates measured in the pulsed electron experiments.^{8,9}

The best way to test the dynamical approximation made in the present work is to compare our results with those of full rotational close-coupling calculations at low energies (Table II). Results from the SP model are seen to be in reasonable agreement with the results of the earlier static-polarization calculations by Itikawa and Takayanagi,¹ even to the pronounced minimum in the cross section for elastic scattering from the ground rotational state at ~ 0.2 eV (this minimum is shifted to ~ 1.0 eV with the inclusion of exchange). Differences that do exist cannot be attributed solely to the different dynamical approximations made, since the present work employs a more elaborate model of the SP interaction potential. Sensitivity to the latter is substantial, as previously noted,¹ and as can be seen by comparing the SP and SMEP results in Table II. The largest difference between our SP results and those of Itikawa and Takayanagi occurs for the $0 \rightarrow 2$ cross section at the higher energies, and, as they first suggested, can be attributed to their neglect of the quadrupole interaction.

Our SP results disagree dramatically, however, with those of Gianturco and Rahman³⁵ in both shape and magnitude. The SP potentials used in the present and latter work being presumably quite similar, this disagreement is much too large to be attributed solely to different dynamical approximations. We suspect, rather, that the latter suffered from an inadequate range of radial integration ($100a_0$, compared with, e.g., $\sim 40/k$ in the work of Itikawa and Takayanagi). We obtained similar results by limiting the range of integration to $100a_0$ (see also Table I). Their conclusion that the elastic cross section dominates below 0.3 eV is not supported by the present or earlier¹ results. They reached a similar conclusion for HF, which is even more suspect since HF has a dipole moment about twice that of HCl.

The relative importance of various contributions

to the total interaction potential is illustrated in Table III. The FBA is seen to be qualitatively correct for the dipole transition over the entire energy range, but for the quadrupole transition only at the highest energies. Thus the results (calculated using $D=0.436$ a.u.) of the semiclassical sudden S -matrix (SSSM) model of Allan and Dickinson³⁶ are also reasonably good for the dipole transition. This model employs a dynamical approximation similar to that made in the present work. The effect of second-order coupling via the dipole interaction is most important for the elastic and quadrupole interaction at low energies, thereby accounting for the qualitatively correct behavior of the results of the SSSM model, in which this is the only effect included. At higher energies the effects of exchange, polarization, and the quadrupole interaction become dominant.

These comparisons give us no reason to seriously doubt the reliability of the dynamical approximation made in the present work. It would appear, rather, that the treatment of the interaction potential is of much greater importance. The fact remains that further rotational close-coupling calculations, employing an interaction potential (SP or SMEP) identical to that used in the present work, would be very useful.

The generally good agreement of the results of our calculations with available measured data for vibrationally elastic scattering encourages us to pursue vibrational excitation. We first intend to complete study of the former with an essentially exact treatment of exchange.²² The obvious importance of polarization at intermediate distances also argues strongly for a more sophisticated treatment of this interaction. Two interesting possibilities in this regard are optical potential approaches³⁷ and a generalization of the free-electron-gas concept to encompass correlation effects.³⁸ Either of these would eliminate the unsatisfactory dependence on an *ad hoc* cutoff parameter, as in (1). In any event, we will require some estimate of the polarizability as a function of internuclear separation. We are fortunate that HCl is one of the few molecules for which this has been studied.³⁹

ACKNOWLEDGMENTS

We wish to thank D. K. Davies and F. Linder for permission to cite their results in advance of publication. This work was supported by the U.S. Department of Energy through the Los Alamos National Laboratory (L.A.C.) and the Office of Basic Energy Sciences (N.T.P. and D.W.N.). One of us (N.T.P.) wishes to thank FAPESP (Fundacao de Amparo a Pesquisa do Estado de Sao Paulo) for support in the early stages of this calculation.

- *On leave from Universidade Estadual de Campinas, Instituto de Física, 13100 Campinas-SP, Brazil.
- †Quantum Physics Division, National Bureau of Standards.
- ¹Y. Itikawa and K. Takayanagi, *J. Phys. Soc. Jpn.* **26**, 1254 (1969).
- ²Y. Itikawa, *J. Phys. Soc. Jpn.* **27**, 444 (1969).
- ³K. Rohr and F. Linder, *J. Phys. B* **8**, L200 (1975).
- ⁴See N. F. Lane, *Rev. Mod. Phys.* **52**, 29 (1980).
- ⁵W. Domcke and L. S. Cederbaum, *J. Phys. B* **14**, 149 (1981).
- ⁶K. Rohr and F. Linder, *J. Phys. B* **9**, 2521 (1976); and personal communication.
- ⁷M. Allan and S. F. Wong, *J. Chem. Phys.* **74**, 1687 (1981).
- ⁸D. Kligler, Z. Rosenberg, and M. Rokni, *Appl. Phys. Lett.* **39**, 319 (1981).
- ⁹R. E. Center, J. H. Jacob, M. Rokni, and Z. Rozenberg, *Appl. Phys. Lett.* **41**, 116 (1982).
- ¹⁰E. Brüche, *Ann. Phys.* **82**, 25 (1972).
- ¹¹D. K. Davies, in proceedings of the 34th Gaseous Electronics Conference, Boston, Mass., 1981 (unpublished), and personal communication.
- ¹²P. A. Cade and W. M. Huo, *J. Chem. Phys.* **47**, 649 (1967).
- ¹³M. A. Morrison, *Comput. Phys. Commun.* **21**, 63 (1980).
- ¹⁴G. B. Schmid, D. W. Norcross, and L. A. Collins, *Comput. Phys. Commun.* **21**, 79 (1980).
- ¹⁵Y. Itikawa and O. Ashihara, *J. Phys. Soc. Jpn.* **30**, 1461 (1971).
- ¹⁶S. Hara, *J. Phys. Soc. Jpn.* **22**, 710 (1967).
- ¹⁷F. de Leeuw and A. Dynamus, *J. Mol. Spectrosc.* **48**, 427 (1973).
- ¹⁸F. A. Gianturco and D. G. Thompson, *J. Phys. B* **10**, L21 (1977); L. A. Collins, R. J. W. Henry, and D. W. Norcross, *J. Phys. B* **13**, 2299 (1980).
- ¹⁹J. H. Williams and R. D. Amos, *Chem. Phys. Lett.* **70**, 162 (1980).
- ²⁰N. J. Bridge and A. D. Buckingham, *Proc. R. Soc. London, Ser. A* **295**, 334 (1966).
- ²¹L. A. Collins, W. D. Robb, and D. W. Norcross, *Phys. Rev. A* **20**, 1838 (1979).
- ²²L. A. Collins and B. I. Schneider, *Phys. Rev. A* **24**, 2387 (1981).
- ²³M. A. Morrison, N. F. Lane, and L. A. Collins, *Phys. Rev. A* **15**, 2186 (1977); L. A. Collins and D. W. Norcross, *ibid.* **16**, 467 (1978).
- ²⁴D. W. Norcross and N. T. Padial, *Phys. Rev. A* **25**, 227 (1982).
- ²⁵Cross sections in the FBA for the dipole transition are well known (see Ref. 4). Forms for transitions governed by the selection rules associated with the Clebsch-Gordan coefficient $C(j, 2, j'; 00)$ that involve both the quadrupole moment and polarizability are easily deduced from the work of A. Dalgarno and R. J. Moffett [*Proc. Natl. Acad. Sci. India* **33**, 511 (1963)].
- ²⁶D. W. Norcross, *Phys. Rev. A* **25**, 764 (1982).
- ²⁷N. T. Padial, D. W. Norcross, and L. A. Collins, *J. Phys. B* **14**, 2901 (1981).
- ²⁸H. S. Taylor, E. Goldstein, and G. A. Segal, *J. Phys. B* **10**, 2253 (1977).
- ²⁹L. Dube and A. Herzenberg, *Phys. Rev. Lett.* **38**, 820 (1977).
- ³⁰R. K. Nesbet, *J. Phys. B* **10**, L739 (1977).
- ³¹M. H. Mittleman and R. E. Von Holdt, *Phys. Rev.* **140**, A726 (1966).
- ³²T. F. O'Malley, *Phys. Rev.* **137**, A1668 (1965).
- ³³A. Hazi and C. W. Clark, personal communication.
- ³⁴T. N. Rescigno, A. E. Orel, A. U. Hazi, and B. V. McKoy, *Phys. Rev. A* **26**, 690 (1982).
- ³⁵F. A. Gianturco and N. K. Rahman, *J. Phys. B* **11**, 727 (1978).
- ³⁶R. J. Allan and A. S. Dickinson, *J. Phys. B* **14**, 1675 (1981).
- ³⁷See, for example, B. I. Schneider and L. A. Collins, *J. Phys. B* (in press).
- ³⁸J. O'Connell and N. F. Lane, *Phys. Rev. A* (in press).
- ³⁹F. A. Gianturco and U. T. Lamanna, *J. Phys. B* **12**, 2789 (1979).